Revised Version

DESY 98-051
LUNFD6/(NFFL-7156) 1998

DESY 98-051 ISSN 0418–9833
LUNFD6/(NFFL-7156) 1998

Resolved photon processes in DIS and small x dynamics.

H. Jung, L. Jönsson, H. Küster

Physics Department, Lund University, P.O. Box 118, 221 00 Lund, Sweden

Abstract

It has been found that recent results on forward jet production from deep inelastic scattering can neither be reproduced by models which are based on leading order α_s QCD matrix elements and parton showers nor by next-to-leading order calculations. The measurement of forward jet cross sections has been suggested as a promising probe of new small x dynamics and the question is whether these data provide an indication of this. The same question arises for other experimental data in deep inelastic scattering at small x which can not be described by conventional models for deep inelastic scattering. In this paper the influence of resolved photon processes has been investigated and it has been studied to what extent such processes are able to reproduce the data. It is shown that two DGLAP evolution chains from the hard scattering process towards the proton and the photon, respectively, are sufficient to describe effects, observed in the HERA data, which have been attributed to BFKL dynamics.

1 Introduction

The cross section of forward jet production in deep inelastic scattering (DIS) has been advocated as a particularly sensitive measure of small x parton dynamics [1, 2]. Analytic calculations based on the BFKL equation in the leading logarithmic approximation (LLA) are in fair agreement with data. However, recent calculations of the BFKL kernel in the next-to-leading logarithmic approximation (NLLA) [3] have given surprisingly large corrections, and it remains to be shown whether the data can still be reasonably described.

Monte Carlo generators based on direct, point-like photon interactions (DIR model), calculated from leading order (order α_s) QCD matrix elements, and leading log parton showers based on the DGLAP evolution do not take any new parton dynamics in the small x region into account and are therefore not expected to fit the experimental data. Recent results from the H1 [4] and ZEUS [5] experiments on forward jet production exhibit significant deviations from the predictions of such models. Also next-to-leading order calculations (NLO i.e. order α_s^2) predict too small a cross section compared to data.

Similarly the DIR model is unable to reproduce the fractional di-jet rate, R_2, as a function of x and Q^2 [6], investigated in a kinematic domain where $p_{T,jet}^2 \gtrsim Q^2$. In these events the two

high p_T jets originate from the hard scattering process. Discrepancies up to a factor of three are observed. Inclusive jet cross sections in the transition region between photo-production and DIS are measured to be significantly larger than predicted by models assuming DGLAP based direct interactions [7].

Measurements of the transverse energy flow [8, 9] do not provide a clear distinction between various models, whereas it has been demonstrated that the data on transverse momentum spectra of charged particles [10] can not be described by conventional leading order DGLAP equations at small x and Q^2, a region where new parton dynamics are expected to become important.

On the other hand all these data samples are rather well described by the color dipole model (CDM) as implemented in the Monte Carlo program ARIADNE [11]. In the CDM the gluon emission is described as radiation from color dipoles stretched between quark-antiquark pairs. These color dipoles radiate independently and therefore the gluons are not ordered in transverse momentum (k_T). This dis-ordering in k_T is also a prominent feature of the BFKL dynamics where the parton emission follows a "random walk" in k_T. The DGLAP evolution used in the DIR model gives strong ordering in k_T. The question is thus whether all these data provide an indication of new small x parton dynamics.

In this work we have studied the possible contribution of virtual resolved photons to the cross section of the DIR model as a possible alternative explanation for the differences between data and the Monte Carlo predictions. All the studies have been performed with the RAPGAP 2.06 [12, 13] Monte Carlo event generator. It has been checked that this generator agrees well with analytical LO calculations and with the LEPTO 6.5 [14] Monte Carlo in the case of direct interactions.

2 Resolved Photons in DIS

In electron-proton scattering the internal structure of the proton as well as of the exchanged photon can be resolved provided the scale of the hard subprocess is larger than the inverse radius of the proton, $1/R_p^2 \sim \Lambda_{QCD}^2$, and the photon, $1/R_\gamma^2 \sim Q^2$, respectively. Resolved photon processes play an important role in photo-production of high p_T jets, where $Q^2 \approx 0$, but they can also give considerable contributions to DIS processes [7, 15] if the scale μ^2 of the hard subprocess is larger than Q^2, the inverse size of the photon.

In the following we give a brief description of the model for resolved virtual photons used in the Monte Carlo generator RAPGAP. Given the fractional momentum transfer of the incoming electron to the exchanged photon, the Equivalent Photon Approximation provides the flux of virtual transversely polarized photons [13, 12, and references therein]. The contribution from longitudinally polarized photons has been neglected. The partonic structure of the virtual photon is defined by parameterizations of the parton densities, $x_\gamma f_\gamma(x_\gamma, \mu^2, Q^2)$, which depend on the two scales μ^2 and Q^2 [16, 17, 18]. The following hard subprocesses are considered (RES model): $gg \to q\bar{q}$, $gg \to gg$, $qg \to qg$, $q\bar{q} \to gg$, $q\bar{q} \to q\bar{q}$, $qq \to qq$. Parton showers on both

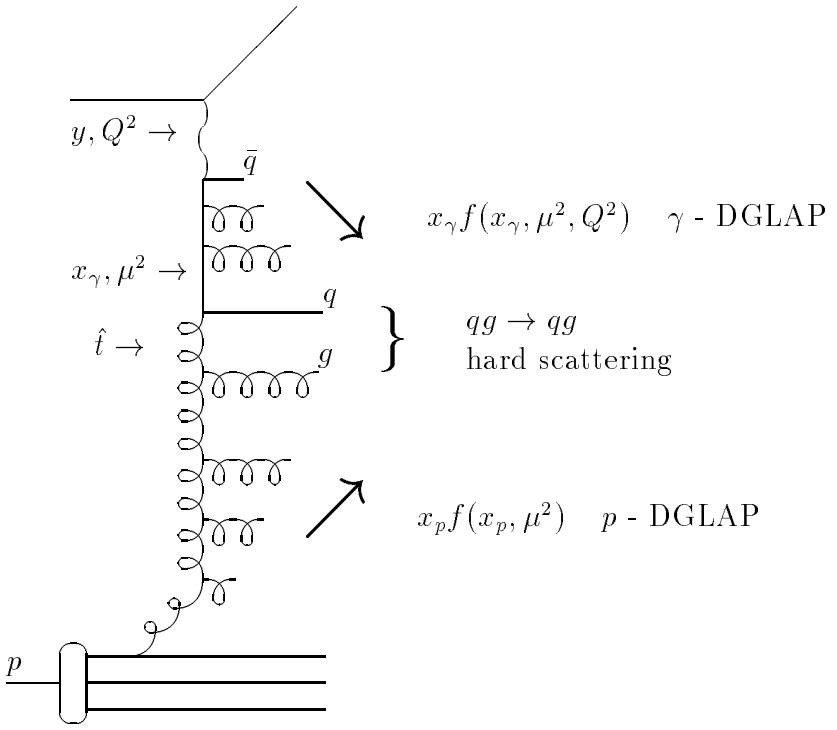

Figure 1: Deep inelastic scattering with a resolved virtual photon and the $q_\gamma g_p \rightarrow qg$ partonic subprocess.

the proton and the photon side are included. The generic diagram for the process $q_\gamma g_p \rightarrow qg$ including parton showers is shown in Fig. 1.

Since the photon structure function depends on the scale, μ^2, of the hard scattering process, the cross section of resolved photon processes will consequently also depend on the choice of this scale. The parton density of the photon is evolved from a starting scale Q_0^2 to the scale μ^2, the virtuality at the hard subprocess, giving a resummation to all orders.

It should be noted that a NLO calculation assuming point-like virtual photons contains a significant part of what is attributed to the resolved structure of the virtual photon in the RES model [19]. This is due to the fact that in order α_s^2 the virtual photon can split into a $q\bar{q}$ pair with one of the two quarks interacting with a parton from the proton, giving rise to two high p_T jets.

2.1 Choice of Scale

In leading order α_s processes the renormalization scale μ_R and factorization scale μ_F are not well defined which allows a number of reasonable choices. There are essentially two competing effects: a large scale suppresses $\alpha_s(\mu^2)$ but gives, on the other hand, an increased parton density, $xf(x, \mu^2)$, for a fixed small x value. The net effect depends on the details of the interaction and on the parton density parameterization.

However, in resolved virtual photon processes the choice of the scale μ^2, at which the photon is probed, is severely restricted [20]. If we proceed from the electron (see Fig. 1) towards the hard subprocess, the first branching occurs already at the electron vertex $e \to e'\gamma^*$, where the scale in DIS is chosen to be $Q^2 = -t$ (t being the Mandelstam variable of a $2 \to 2$ process), which is related to the transverse momentum of the scattered electron by: $Q^2 = p^2_{T;e'}/(1-y)$. Here y is defined by $y = \frac{q.P}{l.P}$, with l and P being the four vectors of the incoming electron and proton and q is the four vector of the (virtual) photon with $q^2 = -Q^2$. This indicates that the scale must be larger than $p^2_{T;e'}$, for a typical value of $y \sim 0.5$, this gives $Q^2 = 2 \cdot p^2_{T;e'}$

Within a consistent picture of the evolution from the electron towards the hard scattering process, the definition of the scale should be kept the same for all branchings. Thus the proper scale for a hard scattering process in the $\hat{t}$ - channel (as shown in Fig. 1) would be $\hat{t}$, since $Q^2 = -t$. Here $\hat{t}$ refers to the hard scattering process. However not only $\hat{t}$ - channel diagrams contribute, but also $\hat{u}$ and $\hat{s}$ - channel diagrams as well as interference terms. The calculation of the relative contributions to the cross section in principally limited due to the interference terms. We are therefore forced to make a best guess of a reasonable scale. We have chosen 2 different scales: $\mu^2 = 4p^2_T$ and $\mu^2 = Q^2 + p^2_T$. The first one is closely related to the $\hat{t}$ - channel diagrams, where we have included a factor of 4 to account for the fact that $|\hat{t}| > p^2_T$. The second one is chosen for a smooth transition from usual DIS to DIS including resolved photons and to photo-production. This choice of scale has also been used in NLO calculations including resolved photons in deep inelastic scattering [19].

2.2 Parton Distribution Functions

Two parameterizations of the parton distribution in the proton, GRV 94 HO (DIS) and CTEQ4M have been considered, which both give good agreement with the proton structure function data [21, 22]. It was found that the produced results were identical within the percent level, when keeping Λ_{QCD} fixed.

Also for the virtual photon two different parameterizations of the parton density have been investigated. The photon can interact via its partons either in a bound vector meson state or as decoupled partons if the p_T of the partons is high enough. Only the latter is relevant in the Q^2 range considered in this paper. The splitting $\gamma \to q\bar{q}$ is called the anomalous component of the photon. The SaS [17] parameterization offers a choice of Q^2_0 values at which the anomalous part becomes effective. We have studied these choices resulting in different magnitudes of the parton densities, and consequently of the cross sections. For the SaS parameterization we have used Q^2_0 as given by eq.(12) of ref. [17] ($IP2 = 2$), which gave the largest resolved photon contribution.

The GRV LO parton density description of the real photon together with the virtual photon suppression factor of Drees and Godbole (DG) [18] gives similar results. Drees and Godbole proposed a x_γ - independent suppression factor:

$$r = 1 - \frac{\log(1 - \frac{Q^2}{P^2_c})}{\log(1 - \frac{\mu^2}{P^2_c})}$$

with an adjustable parameter P_c^2, which is set to $P_c^2 = 0.5$ GeV^2 typical for a hadronic scale. Comparisons between the SaS and the DG parameterizations are given for some of the observables.

The GRS [16] structure function for the virtual photon has not been used, since it is restricted to $Q^2 < 10$ GeV^2 which is not useful for the studies presented here,

If not stated otherwise, in the following we have used the scale $\mu^2 = Q^2 + p_T^2$, the CTEQ4M parameterization of the parton density in the proton and the DG description of the photon.

3 Forward Jets

HERA has extended the available x region down to values below 10^{-4} where new parton dynamics might show up. Based on calculations in the LLA of the BFKL kernel, the cross section for DIS events at low x and large Q^2 with a high p_T^2 jet in the proton direction (a forward jet) [1, 2] is expected to rise more rapidly with decreasing x than expected from DGLAP based calculations. New preliminary results from the H1 [4] and ZEUS [5] experiments have recently been presented. The data can be described neither by conventional DIR Monte Carlo models nor by a NLO calculation, while comparisons to analytic calculations of the LLA BFKL mechanism has proven reasonable agreement.

It should be kept in mind that both the NLO calculations and the BFKL based calculations are performed on the parton level whereas the data are on the level of hadrons. Nevertheless these comparisons make sense, considering the present measuring errors and the fact that simulations have shown that the hadronization effects are at most 20%.

In this study, Monte Carlo events from the RAPGAP generator have been used to investigate whether the experimental data can be equally well reproduced by the inclusion of resolved photon processes. The cuts applied in the laboratory frame are equivalent to those in the preliminary H1 analysis [4].

Kinematic cuts:

$$y > 0.1 \quad (1)$$

$$E_e' > 11\text{GeV} \quad (2)$$

Jet selection:

$$E_{jet} > 28.7 \text{ GeV} \quad (3)$$

$$p_T^{jet} > 3.5 \text{ GeV} \quad (4)$$

$$7^o < \theta_{jet} < 20^o \quad (5)$$

where $\theta = 0^o$ corresponds to the proton beam direction.

Jets were reconstructed in the η-ϕ space by applying a cone algorithm with a cone radius of $R = \sqrt{\eta^2 + \phi^2} = 1$. The jet cuts have been defined to ensure that the momentum fraction of

the jet ($x_{jet} = E_{jet}/E_p$, where E_p is the proton energy) is large compared to x so as to maximize the phase space for a evolution in x. At large x_{jet} the parton distributions of the proton are well measured and the uncertainty from non-perturbative effects is avoided. In order to suppress the phase space for DGLAP evolution, the p_T^2 of the jets was further required to be of the same order of magnitude as Q^2 ($0.5 < p_T^2/Q^2 < 2$). Thus DIS events with small x and an energetic high p_T jet in the forward direction are selected.

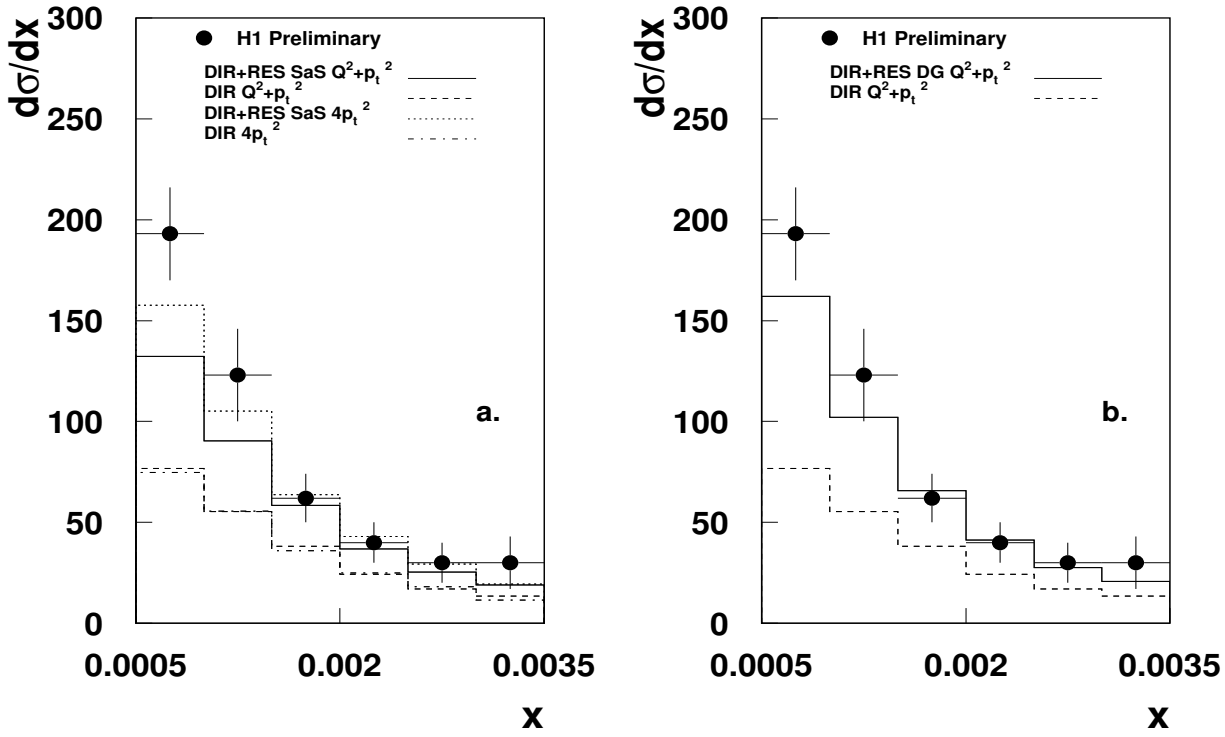

Figure 2: The forward jet cross section as a function of x using the cuts specified in the text. The data points are preliminary H1 data [4]. In *a.* are shown the RAPGAP predictions for the sum of direct and resolved processes using again the scales $\mu^2 = Q^2 + p_T^2$ (solid line) and $\mu^2 = 4p_T^2$ (dotted line). Also included are the predictions for direct DIS processes with the scales $\mu^2 = Q^2 + p_T^2$ (dashed line) and $\mu^2 = 4p_T^2$ (dash-dotted line), respectively. The parton distribution of the virtual photon was parameterized according to SaS 2 DIS. In *b.* the sum of direct and resolved processes (solid line) and the direct (dashed line) are presented using the DG + GRV description of the parton density in the photon and with the scale $\mu^2 = Q^2 + p_T^2$. In all cases the parton density of the proton was described by CTEQ4M.

In Fig. 2 the preliminary data of the H1 collaboration [4] are compared to the RAPGAP Monte Carlo predictions for both, direct process alone (labeled DIR) and for the sum of direct

and resolved processes (labeled DIR+RES). The comparison is performed for the two scales, $\mu^2 = Q^2 + p_T^2$ and $\mu^2 = 4p_T^2$ and for the two parameterizations of the photon parton density (SaS, Fig. 2a, and DG, Fig. 2b). It is clearly seen that the direct contribution alone is not sufficient to reproduce the data whereas the DIR+RES model gives good agreement with data. The scale $\mu^2 = 4p_T^2$ seems to give a slightly better agreement with data than the scale $\mu^2 = Q^2 + p_T^2$ for the SaS photon structure function whereas for the DG photon structure function the scale $\mu^2 = Q^2 + p_T^2$ leads to a good description of data and $\mu^2 = 4p_T^2$ results in predictions which overshoot the data (not shown). This simply illustrates the uncertainty in the scale and in the parameterization of the photon structure function. The hard process $q_\gamma g_p \to qg$ contributes most to the forward jet cross section.

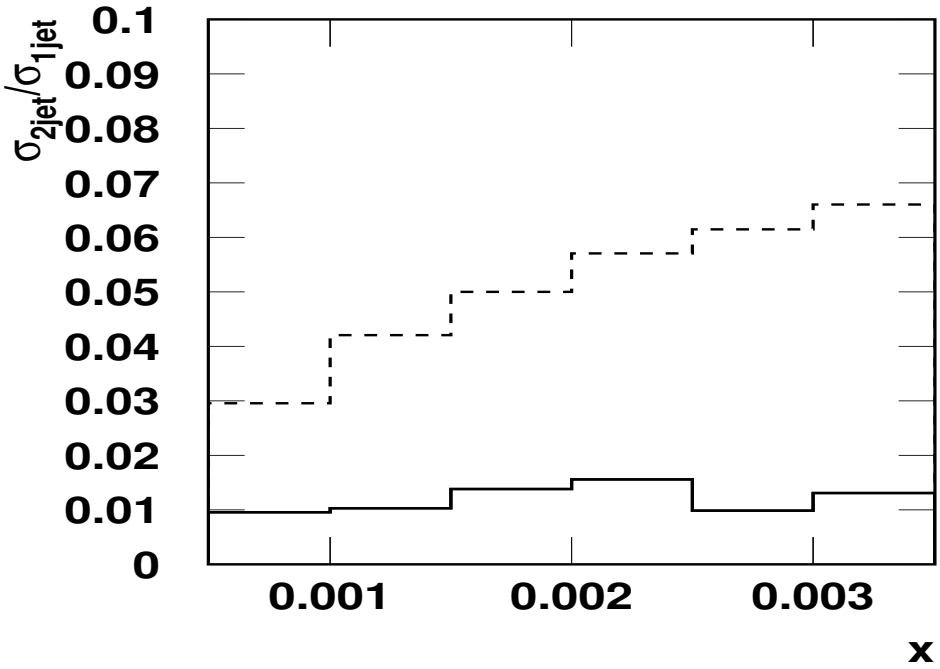

Figure 3: The ratio of cross sections for the production of two and one forward jets versus x, as predicted by the RAPGAP Monte Carlo for the sum of direct and resolved processes (solid line). The cuts applied are specified in the text. The prediction from the analytical calculation of [23] is shown with the dashed line.

A small fraction of the DIS events, fulfilling the selection criteria for forward jets, actually contains two identified jets. The ratio of the cross sections for events with two and one forward jet(s) would be a measure of the BFKL vertex function which controls the emission of the second

jet. Analytic calculations (in LLA) [23] have been performed in the same kinematic region and with the same jet selection as defined above for the one-jet sample. The predicted ratio varies from 3% to 6%, for a cone radius of $R = 1$, when going from $x = 0.5 \cdot 10^{-3}$ to $x = 3 \cdot 10^{-3}$. Comparisons to experimental data are not yet available. The prediction of the RAPGAP Monte Carlo for direct plus resolved processes is shown in Fig. 3. It is about a factor of 3 lower than the prediction from the BFKL calculations. A large part of this discrepancy could be due to hadronization effects which would reduce the prediction of the parton level BFKL calculation. Given the large uncertainties both in the resolved photon and BFKL calculations, it is not obvious that the two approaches give results in the same order of magnitude.

4 Other tests of low x dynamics

In this section we discuss measurements like the (2 + 1) jet rate in DIS, transverse energy flow and the p_T spectra of charged particles, which are not well described by DIR models and have been subject to speculations on their possible interpretation in terms of small x BFKL dynamics.

4.1 Di-jet rates in DIS

New H1 data on fractional di-jet rates were recently made public [6]. Events with two jets were selected in the kinematic region $5 \lesssim Q^2 \lesssim 100$ GeV^2 and $10^{-4} \lesssim x \lesssim 10^{-2}$. The jets were defined in the hadronic center-of-mass system using a cone algorithm of radius $R = 1$ and requiring a transverse momentum $p_T^{jet} > 5$ GeV. The results make evident that standard DIR LO Monte Carlo models such as RAPGAP 2.06 in the direct mode and LEPTO 6.5 badly fail to describe the data. Especially in the Q^2 region below 30 GeV^2 the discrepancies are large but in this region $p_T^2 > Q^2$ and therefore resolved photon interactions are expected to play a significant role. The CDM, on the other hand, gives very good agreement with data.

With the same cuts as in the H1 analysis, RAPGAP has been used, with and without resolved photon processes included, to predict the di-jet rates.

The data from H1 are shown as a function of Q^2 and x in Figs. 4 a) and b), respectively, together with the predictions from RAPGAP. The RAPGAP results on direct and direct+resolved processes are shown separately for the two scales mentioned above and for the two parameterizations of the photon structure. The data are well above the direct contribution, but adding the direct and resolved contributions gives a remarkably good description of data all the way down to the phase space region where the resolved processes are dominating, especially with the scale $\mu^2 = 4p_T^2$ ($\mu^2 = Q^2 + p_T^2$) and the SaS (DG) parameterization of the photon structure. Also in this data sample the major contribution is coming from the $q_\gamma g_p \to qg$ subprocess.

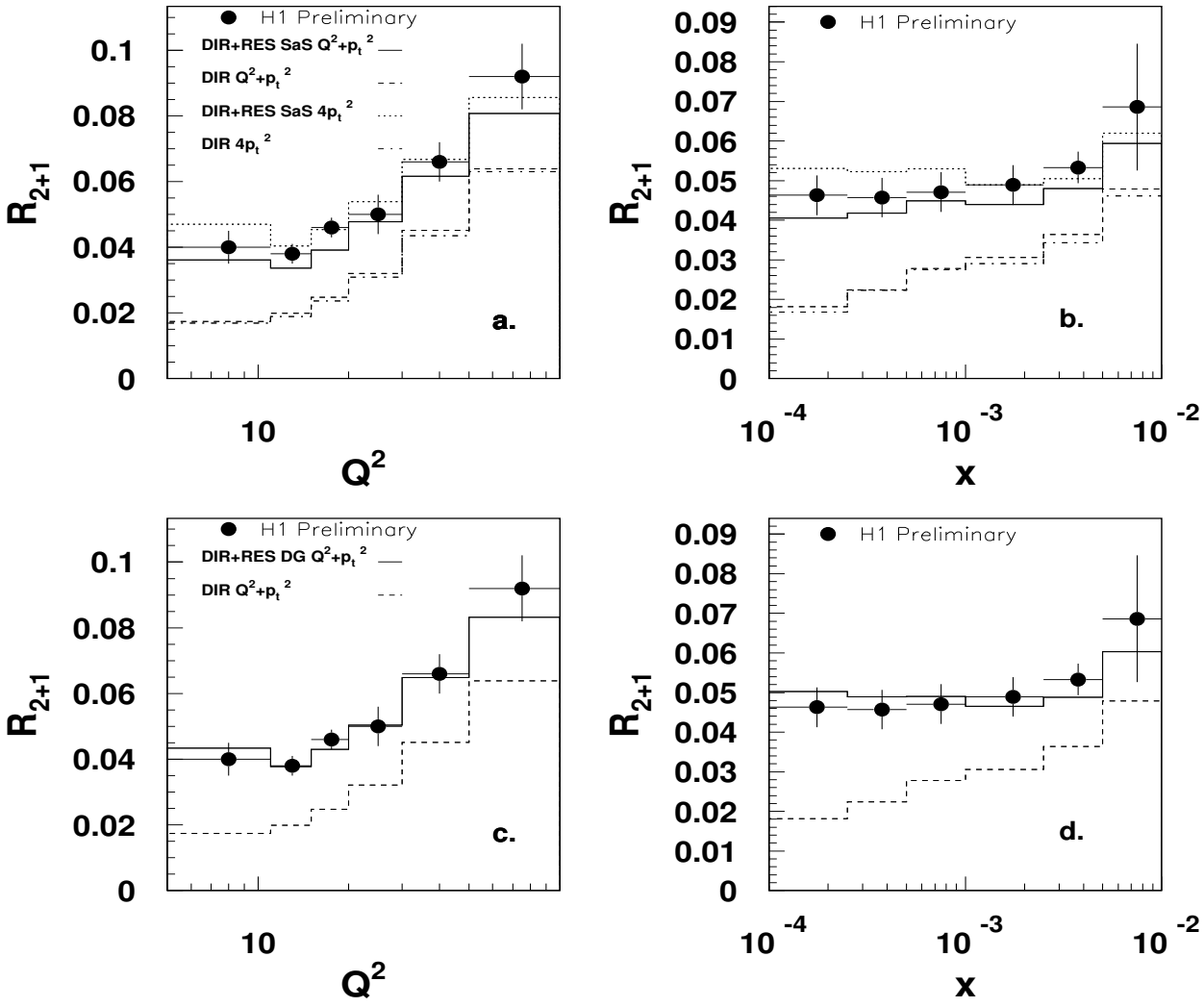

Figure 4: The di - jet ratio R_{2+1} as a function of Q^2 ($a.$ and $c.$) and x ($b.$ and $d.$). The points are preliminary H1 data [6]. In $a.$ and $b.$ are shown the RAPGAP predictions for the sum of direct and resolved processes using the scales $\mu^2 = Q^2 + p_T^2$ (solid line) and $\mu^2 = 4p_T^2$ (dotted line), as well as the predictions for direct processes with the scales $\mu^2 = Q^2 + p_T^2$ (dashed line) and $\mu^2 = 4p_T^2$ (dashed-dotted line). The SaS 2 DIS parameterization was used to describe the parton density in the virtual photon. In $c.$ and $d.$ the sum of direct and resolved processes (solid line) and the direct (dashed line) are presented using the DG description of the parton density in the photon with the scale $\mu^2 = Q^2 + p_T^2$. The parton density of the proton is given in all cases by the CTEQ4M parameterization.

4.2 Inclusive jet production

The H1 experiment has measured the single inclusive jet cross section in a range of photon virtualities from $Q^2 = 0$ to 50 GeV^2 using the k_T cluster algorithm in the hadronic CMS [7]. The jets from DIS processes were required to have transverse momenta above 4 GeV/c. Fig. 5 shows the inclusive jet cross section as a function of Q^2 in bins of E_T together with the predictions of the DIR model and DIR+RES model. In the region where $Q^2 \gtrsim E_T^2$ the DIR model is expected to be valid since the photon can not be resolved. It is found that the DIR model approaches the data as Q^2 increases whereas in the low Q^2 region the deviations become significant. The DIR+RES model gives reasonable agreement with data in the full kinematic range investigated.

4.3 Transverse energy flow

The non ordered k_T parton emissions in low x BFKL dynamics produce more transverse energy than the standard DGLAP evolution scheme in the central rapidity region in the hadronic CMS, which corresponds to the forward region in the laboratory system ($\theta \approx 10^o$). Results from H1 [9] on the transverse energy flow, presented in the hadronic CMS as a function of the pseudo-rapidity, η^*, are shown in Fig. 6 for the kinematic region 3 GeV$^2 < Q^2 < 70$ GeV^2 and $8 \cdot 10^{-5} < x < 7 \cdot 10^{-3}$.

The largest difference between LLA BFKL and standard DGLAP calculations are expected at small x and central rapidities η^*. Discrepancies between data and the DIR model of refs. [8, 24] are also observed in this kinematic region. Only after including a proper treatment of the parton dynamics of the proton remnant in the sea quark scattering processes [14] and using a rather low cutoff on the gluon emission for the parton cascade, a reasonable agreement is achieved with the exception of the lowest x and Q^2 region (see Fig. 6). However the description is significantly improved by including the contribution of resolved virtual photons giving an excellent description of the transverse energy flow over the full range of x and Q^2 as illustrated in Fig. 6. Different scales μ^2 or the parton distribution functions give changes of the order of 5%.

4.4 p_T spectra of charged particles

Studies based on QCD models have demonstrated that the high p_T tail of charged particle transverse momentum spectra is sensitive to small x dynamics of parton radiation and that the influence from hadronization is small [25, 26]. The LLA BFKL dynamics result in harder p_T spectra than obtained in the DGLAP scenario because of the non-ordered k_T emissions. A LLA BFKL based calculation [27] including an estimation of the fragmentation effects was able to reproduce the high p_T tail in the lowest x bins.

Fig. 7 shows the p_T distributions of charged particles as measured by the H1 collaboration [10] for DIS events with 3 GeV$^2 < Q^2 < 70$ GeV^2 in the rapidity range $0.5 < \eta < 1.5$. The

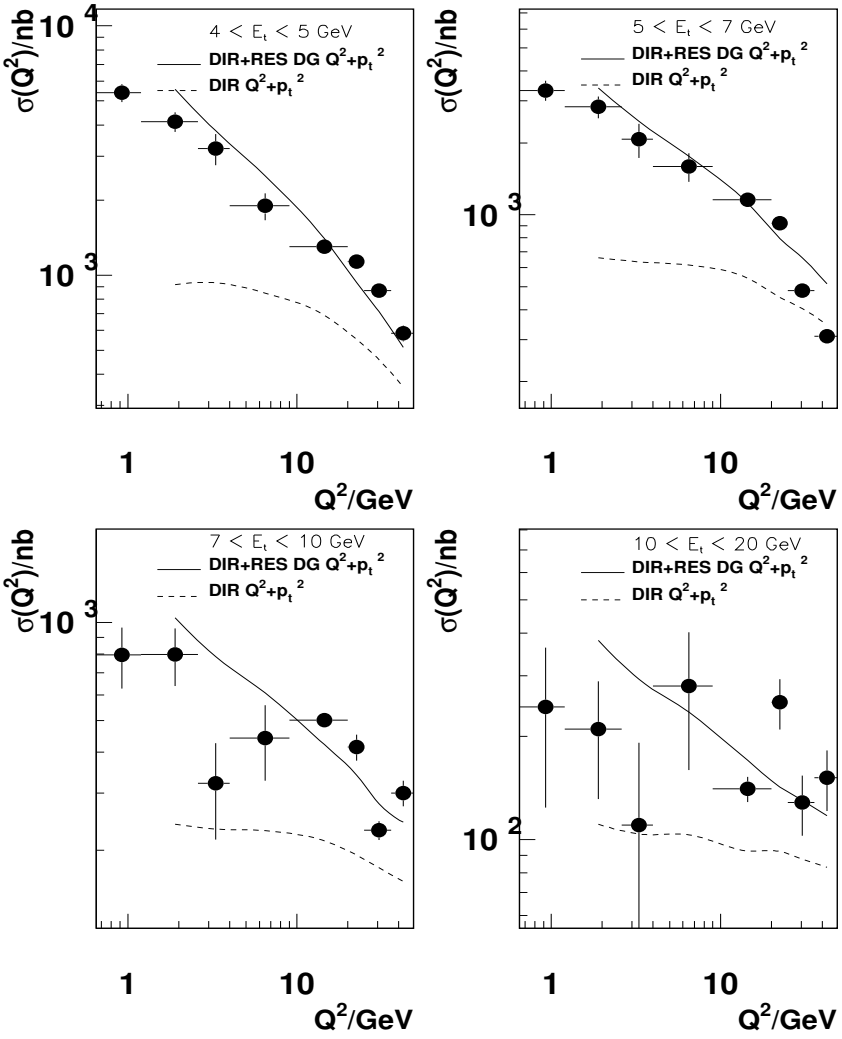

Figure 5: The inclusive jet cross section as a function of Q^2 for different regions of the jet E_T. The points are published H1 data [7], the curves represent the RAPGAP predictions for the sum of direct and resolved processes (solid line) and for direct processes only (dashed line).

H1 analysis [10] showed that both, direct models and CDM provide good agreement with the data at large x, whereas with decreasing x the direct models start falling below the data. In Fig. 7 the dashed line shows the prediction of the DIR model and the solid line the prediction of the DIR+RES model as calculated with the RAPGAP Monte Carlo program. The solid line in Fig. 7 demonstrates a good description of the data over the full range in x and Q^2.

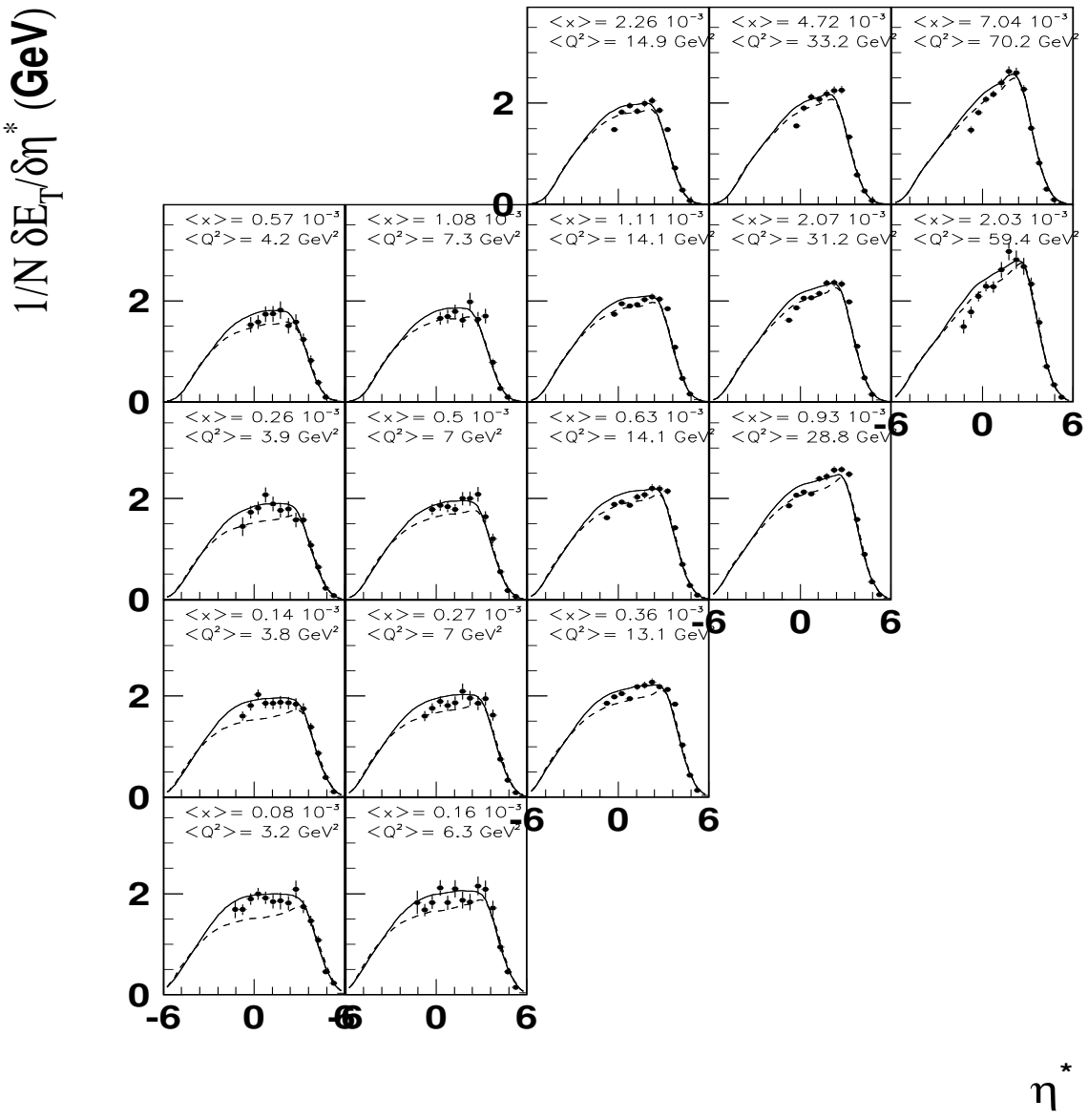

Figure 6: The transverse energy flow as a function of η^* in the hadronic CMS for different bins in Q^2 and x. The data points are preliminary H1 results [9]. Negative η^* corresponds to the proton fragmentation region. The curves give the RAPGAP predictions for the sum of direct and resolved processes (solid line) and for the direct contribution only (dashed line).

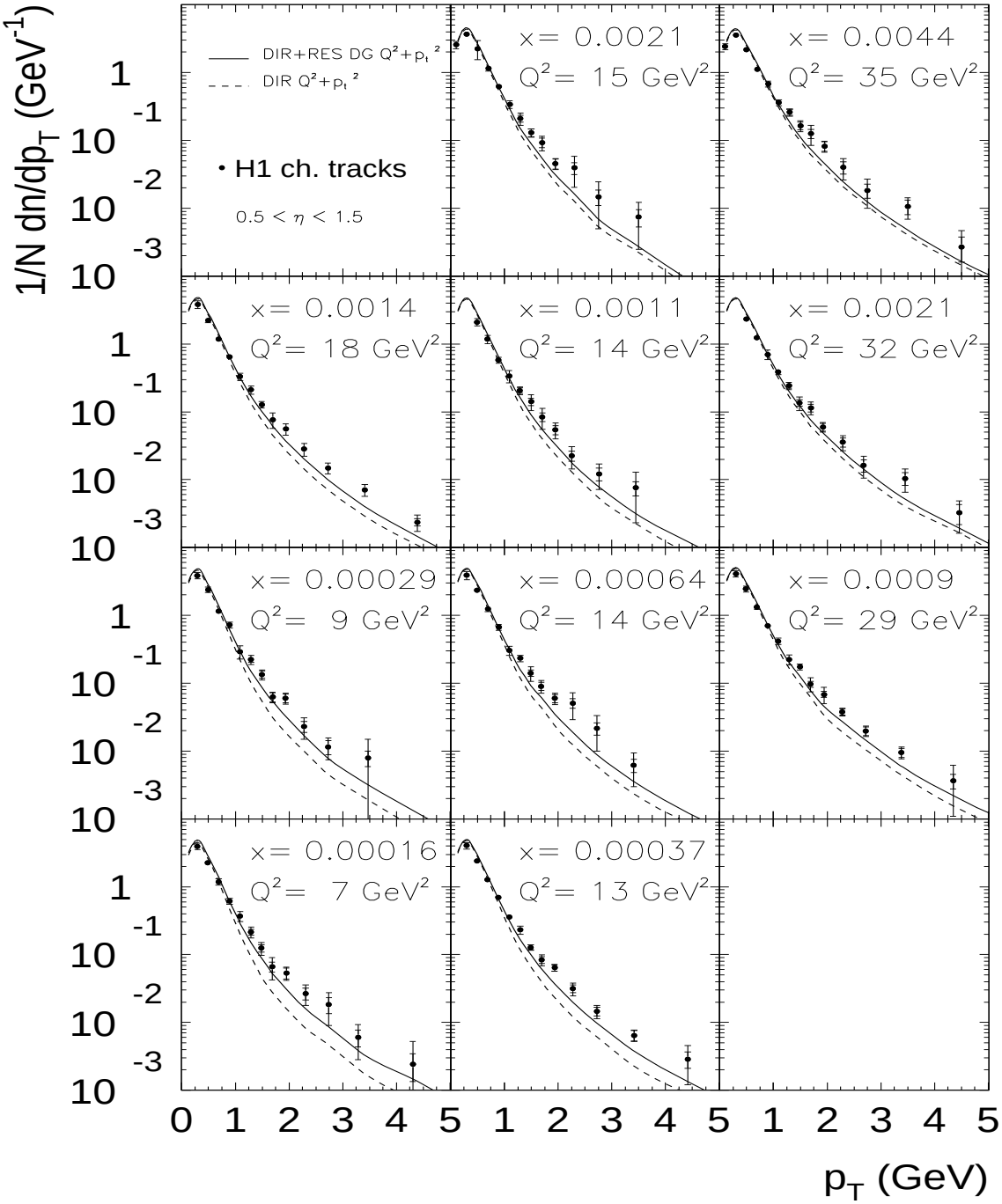

Figure 7: Transverse momentum distributions of charged particles in the rapidity range $0.5 < \eta^* < 1.5$ in the hadronic CMS in bins of Q^2 and x as obtained by H1 [10]. The RAPGAP prediction for direct processes (dashed line) and for the sum of direct and resolved photon contributions (solid line) are shown for comparison.

5 Discussion

Recent experimental data on forward jet production show deviations from traditional LO Monte Carlo models assuming directly interacting point-like photons. This has given rise to various speculations. Similar deviations have been observed in other measurements like the fractional di-jet rates, inclusive jet production, transverse energy flow and in the transverse momentum spectra of charged particles. It is tempting to assume that the observed effects could be explained by BFKL dynamics as firstly the data on forward jet production, which has been proposed as a possible probe of low x dynamics, can not be reproduced by the DGLAP evolution and secondly that the CDM MC, which produces radiation without ordering in k_T as expected for BFKL, reproduces all data fairly well.

In the present study it has been shown that the addition of resolved photon processes to the direct interactions in DIS leads to good agreement with the data, without invoking any BFKL parton dynamics. We have observed that the dominant contributions to the resolved photon processes come from order α_s^2 diagrams with the hard subprocess $q_\gamma g_p \to qg$ (see Fig. 1). Since the partons which form the photon remnant per definition have smaller p_T than the partons involved in the hard scattering, a situation with non k_T ordering is created.

In the LO DIR model the ladder of gluon emissions is governed by DGLAP dynamics giving a strong ordering of k_t for emissions between the photon and the proton vertex. The models describing resolved photon processes and BFKL dynamics are similar in the sense that both lead to a breaking of this ordering in k_t. The BFKL picture, however, allows for complete dis-ordering in k_t, while in the resolved photon case the DGLAP ladder is split into two shorter ladders, one from the hard subsystem to the proton vertex, and one to the photon vertex, each of them ordered in k_t (see Fig. 1). Only if the ladders are long enough to produce additional hard radiation it might be possible to separate resolved photon processes from processes governed by BFKL dynamics. Thus the resolved photon approach may be a "sufficiently good" approximation to an exact BFKL calculation and the two approaches may prove indistinguishable within the range of x accessible at HERA.

It should be emphasized again that a NLO calculation assuming point-like virtual photons contains a significant part of what is attributed to the resolved structure of the virtual photon in the RES model [19].

6 Acknowledgments

It is a pleasure to thank G. Ingelman and A. Edin for discussions about the concept of resolved photons. We have also profited from a continuous dialogue with B. Andersson, G. Gustafson and T. Sjöstrand. We want to thank G. Kramer and B. Pötter for many discussions on the relation between resolved photons in DIS and its relation to NLO calculations. We are grateful to J. Gayler for careful reading of the manuscript and for clarifying comments. We also want to thank M. Wüsthoff and J. Bartels for discussions on BFKL and the resolved photons in DIS.

References

[1] A. Mueller, *Nucl. Phys.* **B** *(Proc. Suppl)* **18C** (1990) 125.

[2] A. Mueller, *J. Phys.* **G 17** (1991) 1443.

[3] V. Fadin, L. Lipatov, BFKL pomeron in the next-to-leading approximation, hep-ph/9802290 .

[4] H1 Collaboration, C. Adloff et al., Contributed paper, pa 03-49, ICHEP96, Warsaw, Poland, July 1996 (unpublished).

[5] ZEUS Collaboration; J.Breitweg et al., Forward Jet Production in Deep Inelastic Scattering at HERA, 1998, DESY 98-050.

[6] H1 Collaboration, T. Ahmed et al., Contributed paper, Abstract 247, HEP97, Jerusalem, Israel, August 1997 (unpublished).

[7] H1 Collaboration, C. Adloff et al., *Phys. Lett.* **B 415** (1997) 418, DESY-97-179.

[8] H1 Collaboration, I. Abt et al., *Z. Phys.* **C 63** (1994) 377, DESY-94-33.

[9] H1 Collaboration, C. Adloff et al., Contributed paper, pa 02-073, ICHEP96, Warsaw, Poland, July 1996 (unpublished).

[10] H1 Collaboration, C. Adloff et al., *Nucl. Phys.* **B 485** (1997) 3, DESY-96-215.

[11] L. Lönnblad, *Comp. Phys. Comm.* **71** (1992) 15.

[12] H. Jung, *Comp. Phys. Comm.* **86** (1995) 147.

[13] H. Jung, *The RAPGAP Monte Carlo for Deep Inelastic Scattering, version 2.06*, Lund University, 1998, \protect\vrule width0pt\protect\href{http://www-h1.desy.de\string~jung/rapgap.html}{

[14] G. Ingelman, A. Edin, J. Rathsman, *Comp. Phys. Comm.* **101** (1997) 108.

[15] J. Chyla, J. Cvach, Virtual Photon Structure from jet production at HERA, in *Proc. of the Workshop on Future Physics at HERA*, edited by G. Ingelman, A. De Roeck, R. Klanner (Hamburg, 1996).

[16] M. Glück, E. Reya, M. Stratman, *Phys. Rev.* **D 54** (1996) 5515.

[17] G. Schuler, T. Sjöstrand, *Phys. Lett.* **B 376** (1996) 193.

[18] M. Drees, R. Godbole, *Phys. Rev.* **D 50** (1994) 3124.

[19] G. Kramer, B. Potter, Low Q^2 jet production at HERA in Next-to-Leading Order QCD, hep-ph/9804352 .

[20] G. Gustafson and T. Sjöstrand, private communications 1997 (unpublished).

[21] H1 Collaboration; C. Adloff et al., *Nucl. Phys.* **B 497** (1997) 3, hep-ex/9703012.

[22] ZEUS Collaboration; J.Breitweg et al., *Phys. Lett.* **B 407** (1997) 432, DESY 97-135.

[23] J. Kwiecinski, C. A. M. Lewis, A. D. Martin, *Phys. Rev.* **D57** (1998) 496, hep-ph/9707375.

[24] G. Ingelman, LEPTO 6.1 The Lund Monte Carlo for deep inelastic lepton-nucleon scattering, in *Proc. of the Workshop Physics at HERA (1991) Vol. 3, 1366*, edited by W. Buchmüller, G. Ingelman (DESY, Hamburg, 1991).

[25] M. Kuhlen, *Phys. Lett.* **B 382** (1996) 441, hep-ph/9606246.

[26] M. Kuhlen, High p_t particles in the forward region at HERA, in *Proc. of the Workshop on Future Physics at HERA*, edited by G. Ingelman, A. De Roeck, R. Klanner (DESY, Hamburg, 1996), p. 606, hep-ex/9610004.

[27] J. Kwiecinski, S. C. Lang, A. D. Martin, Single particle spectra in deep inelastic scattering as a probe of small x dynamics, hep-ph/9707240 .